Codon and mRNA sequence optimization of microdystrophin transgenes improves expression and physiological outcome in dystrophic mdx mice following AAV2/8 gene transfer.

Helen Foster[1], Paul S. Sharp[2], Takis Athanasopoulos[1], Capucine Trollet[1] Ian R. Graham[1], Keith Foster[1], Dominic J. Wells[2] & George Dickson[1]

1. Centre for Biomedical Sciences, Royal Holloway College, University of London, Egham, UK

2. Dept. Cellular & Molecular Neuroscience, Faculty of Medicine, Imperial College London, UK

Correspondence should be addressed to:

George Dickson

Chair of Molecular Cell Biology,

School of Biological Sciences,

Royal Holloway - University of London,

Egham, Surrey, TW20 0EX, UK.

Direct Tel: 44-(0)1784-443545

Fax: 44-(0)1784 414224

Email: g.dickson@rhul.ac.uk

Short title: Codon optimisation of microdystrophin improves outcome in mdx.

Abstract:

Duchenne muscular dystrophy is a fatal muscle wasting disorder. Lack of dystrophin compromises the integrity of the sarcolemma and results in myofibres that are highly prone to contraction induced injury. rAAV mediated dystrophin gene transfer strategies to muscle for the treatment of DMD have been limited by the small cloning capacity of rAAV vectors and high titres needed to achieve efficient systemic gene transfer. Here we assess the impact of codon optimisation on microdystrophin (ΔAB/R3-R18/ΔCT) expression and function in the mdx mouse and compare the function of two different configurations of codon-optimised microdystrophin genes (ΔAB/R3-R18/ΔCT & ΔR4-R23/ΔCT), under the control of a muscle restrictive promoter (Spc5-12). Codon optimisation of microdystrophin significantly increases levels of microdystrophin mRNA and protein following intramuscular and systemic administration of plasmid DNA or rAAV2/8. Physiological assessment demonstrates that codon optimisation of ΔAB/R3-R18/ΔCT results in significant improvement in specific force, but does not improve resistance to eccentric contractions compared to non-codon-optimised ΔAB/R3-R18/ΔCT. However, codon-optimised microdystrophin ΔR4-R23/ΔCT completely restored specific force generation and provided substantial protection from contraction induced injury. These results demonstrate that codon optimisation of microdystrophin under the control of a muscle specific promoter can significantly improve expression levels such that reduced titres of rAAV vectors will be required for efficient systemic administration.

Introduction:

Duchenne muscular dystrophy (DMD) is a severe muscle wasting disorder caused by a lack of dystrophin protein in skeletal muscle. Loss of dystrophin compromises the integrity of the muscle cell membrane and results in muscle fibres that are highly prone to contraction induced injury. Consequently there are progressive rounds of degeneration and regeneration of the muscle leading to the replacement of muscle fibres with non-contractile fibrotic tissue and fatty infiltrates. Recent reports have suggested that a minimum of 30% of normal dystrophin levels need to be present uniformly in all myofibres to prevent muscular dystrophy in humans, which is supported by data from transgenic mdx mice (1, 2). Efficient systemic gene transfer of dystrophin is crucial if restoration of muscle function is to be achieved.

Recombinant adeno-associated viral (rAAV) vectors are being investigated intensively for their potential to restore dystrophin expression in dystrophic muscle and thereby improve muscle function and stabilise or halt disease progression (3-7). Two main hurdles exist in the use of rAAV vectors for DMD gene therapy; the packaging capacity of rAAV vectors and the very high titres of rAAV that have been required to achieve efficient systemic administration (6, 7). To overcome the first issue, ‘microgenes’ encoding for truncated microdystrophin proteins have been engineered and tested rigorously in dystrophic mouse muscle (4, 8, 9). A number of these microdystrophin proteins have been demonstrated to improve, but not completely normalise, a range of markers of the dystrophic phenotype. Restoration of the dystrophin associated protein complex (DAPC), stabilisation of muscle degeneration and improvements in muscle

function have been demonstrated following delivery of microdystrophin at different stages of disease progression (6, 10, 11). However, microdystrophin proteins are less able to protect dystrophic muscle from contraction induced injury (7, 8, 10).

Secondly, although much progress has been made in the systemic delivery of rAAV microdystrophin vectors, this success has been achieved with the use of constitutive viral promoters driving gene expression and the injection of very high titres of rAAV. Although such systems are invaluable in a research setting, it will be necessary to develop rAAV vectors that can achieve efficient gene transfer and expression at lower viral titres with a muscle restrictive promoter driving microdystrophin expression that will be more applicable for use in a clinical setting.

In this study, we tested the hypothesis that the optimisation of codon usage within the microdystrophin gene would result in increased levels of transgene expression such that the viral dose needed for effective reconstitution of dystrophin could be reduced. In contrast to treatment with non-codon-optimised rAAV2/8 microdystrophin, mdx mice treated with codon-optimised rAAV2/8 microdystrophin showed increased numbers of dystrophin positive fibres, improved muscle function and amelioration of dystrophic pathology. In addition, we demonstrate that systemic administration of codon-optimised rAAV2/8 microdystrophin under the control of a muscle restrictive promoter can result in skeletal muscle expression at doses of $3x10^{11}$vg/mouse ($1x10^{13}$vg/kg).

Results:

Codon optimisation of microdystrophin increases mRNA and protein levels following plasmid gene transfer.

To assess the impact of codon optimisation on microdystrophin expression, plasmids expressing either non codon-optimised human ΔAB/R3-R18/ΔCT, codon-optimised human ΔAB/R3-R18/ΔCT or codon-optimised human ΔR4-R23/ΔCT were transfected into HEK293T cells and total RNA was collected 48 hours post transfection. Quantitative RT-PCR demonstrates that microdystrophin mRNA levels are increased up to 30-fold ($p<0.05$) following transfection with codon-optimised constructs compared to the control plasmid (**Figure 1a**). These plasmids were also tested in vivo by electrotransfer into the muscle of 6-8 week old mdx mice. Histological analysis of the tibialis anterior (TA) muscles at 7 days post injection demonstrates that treatment with a codon-optimised microdystrophin plasmid significantly increases the number of dystrophin positive fibres compared to a non codon-optimised microdystrophin ($p<0.05$). No difference is observed between codon-optimised ΔAB/R3-R18/ΔCT and ΔR4-R23/ΔCT when comparing levels of mRNA and dystrophin positive fibres (**Figure 1a-b**). Electrotransfer with codon-optimised ΔAB/R3-R18/ΔCT and ΔR4-R23/ΔCT achieves robust staining of microdystrophin at the sarcolemma, although cytoplasmic staining of microdystrophin was observed with ΔR4-R23/ΔCT but not with ΔAB/R3-R18/ΔCT (**Figure 1c-d**).

Codon optimisation of microdystrophin leads to efficient systemic gene transfer at low titres of rAAV2/8.

The impact of codon optimisation on rAAV based gene therapy was assessed, as despite the development of novel serotypes of rAAV, very high titres of rAAV are currently required to achieve efficient systemic gene transfer to the skeletal muscle (7, 12). $3x10^{11}$vg of rAAV2/8 expressing either ΔAB/R3-R18/ΔCT or codon-optimised ΔAB/R3-R18/ΔCT and ΔR4-R23/ΔCT was delivered via the tail vein of young adult mdx mice (10 weeks old). Cardiac and skeletal muscles were recovered at 12 weeks post treatment and assessed histologically.

Following systemic administration of rAAV2/8 ΔAB/R3-R18/ΔCT vectors, codon optimisation was observed to have a significant impact on the number of dystrophin positive cardiomyocytes detected in cardiac muscle ($p<0.001$). However, treatment with codon-optimised ΔR4-R23/ΔCT resulted in levels of dystrophin expression in the cardiac tissue at significantly higher levels than achieved with treatment of any other microdystrophin ($p<0.001$) (**Figure 2**). Further assessment demonstrates that administration of rAAV2/8 vectors expressing ΔAB/R3-R18/ΔCT does not result in notable levels of dystrophin expression with any of the skeletal muscles analysed and that codon optimisation has no impact on this. However, systemic administration of rAAV2/8 vectors expressing codon-optimised ΔR4-R23/ΔCT results in marked dystrophin expression in the skeletal muscle, most notably in the gastrocnemius muscle group, with expression also observed within the diaphragm (**Figure 3**).

Codon optimisation of microdystrophin leads to greater improvements in mdx muscle pathology.

Intramuscular injection of neonatal mdx mice with $7.5x10^9$ vg of rAAV2/8 expressing either codon-optimised human ΔAB/R3-R18/ΔCT, ΔR4-R23/ΔCT or non-codon-optimised ΔAB/R3-R18/ΔCT under the control of the muscle specific promoter Spc5-12, results in sustained expression of microdystrophin for at least 8 weeks (end of experiment), with no evidence of an immune response to the human transgene. Microdystrophin is correctly localised to the sarcolemma and as has previously been demonstrated restores localisation of the DAPC. As was observed following electrotransfer much greater numbers of dystrophin positive fibres can be achieved following treatment with a codon-optimised construct compared to a control microdystrophin construct (ΔAB/R3-R18/ΔCT). However, unlike following electrotransfer, the number of dystrophin positive fibres observed following treatment with codon-optimised ΔR4-R23/ΔCT is vastly superior to treatment with codon-optimised ΔAB/R3-R18/ΔCT, with no evidence of cytoplasmic staining, making these treated muscles difficult to distinguish from wild type muscles (**Figure 4a-h**). In accordance with these observations, central nucleation, a marker of myofibre regeneration, is normalised in muscles treated with codon-optimised ΔR4-R23/ΔCT, but is not improved compared to mdx following treatment with ΔAB/R3-R18/ΔCT (**Figure 5a**). Young adult mdx mice exhibit increased muscle mass compared to age matched controls; treatment with control rAAV2/8 ΔAB/R3-R18/ΔCT has no effect on mass, whilst treatment with codon-optimised ΔAB/R3-R18/ΔCT reduces TA mass significantly ($p<0.05$), but is still greater than wild type controls. However, administration of rAAV2/8 ΔR4-R23/ΔCT reduces the

mass of the mdx TA to such an extent that there is no significant difference to wild type muscle ($p=0.8$; **Figure 5b**).

Delivery of rAAV2/8 codon-optimised microdystrophin leads to greater improvements in mdx muscle function.

Morphological changes in skeletal muscle of the mdx mouse are due to the lack of dystrophin and the deleterious effect that this has on muscle function. To test the ability of microdystrophin constructs to improve muscle function, we administered $7.5x10^9$ vector genomes of a rAAV2/8 expressing either ΔAB/R3-R18/ΔCT or codon-optimised ΔAB/R3-R18/ΔCT or ΔR4-R23/ΔCT under the control of the muscle specific promoter Spc5-12, into the TA muscle of 5 day old mdx mice. Mdx mice typically exhibit an increased maximal tetanic force, but a reduced specific force (force normalised for cross sectional area of the muscle) compared to age matched controls. Injection of rAAV2/8 ΔAB/R3-R18/ΔCT had no effect on either maximal tetanic or specific force compared to untreated mdx. However, specific force was significantly improved following treatment with codon-optimised rAAV2/8 ΔAB/R3-R18/ΔCT ($p<0.01$), but was still reduced compared to wild type mice. In comparison, treatment with codon-optimised rAAV2/8 ΔR4-R23/ΔCT normalised maximal tetanic force, such that specific force was improved significantly compared to mdx mice ($p<0.001$), and showed no difference to the specific force generated by wild type mice (**Figure 6a-c**).

In addition, we tested the ability of codon-optimised microdystrophins to protect mdx myofibres from exercise induced damage, by assessing maintenance of force

production following a series of eccentric contractions. Treatment with either rAAV2/8 ΔAB/R3-R18/ΔCT or the codon-optimised construct was unable to protect mdx muscle from force deficit induced by eccentric contractions (**Figure 7**). However, treatment with codon-optimised rAAV2/8 ΔR4-R23/ΔCT provided substantial protection from force deficit over a series of 10 eccentric contractions (compared to untreated mdx $p<0.001$). In addition, the force deficit curve produced by muscles treated with codon-optimised ΔR4-R23/ΔCT does not show a significant difference compared to the curve produced by wild type muscles ($p=0.31$; **Figure 7**).

Discussion:

This study has focused on the application of codon optimisation of a eukaryotic gene under the control of a muscle restrictive promoter to enhance gene expression and therefore functionality following plasmid and rAAV gene transfer. Both plasmid and rAAV gene transfer are being intensively investigated as potential therapeutic avenues for the treatment of DMD. Key to both these strategies is the ability to deliver the transgene efficiently to skeletal and cardiac muscle to produce robust levels of dystrophin expression under the control of a muscle restrictive promoter. In the case of rAAV, this must be achieved at viral doses that are not prohibitive. Here, we have optimised the codon usage of two different microdystrophin cDNA sequences and compared their expression and functionality to each other, and to a non-codon-optimised control.

Microdystrophin cDNA sequences were optimised in a number of ways to improve mRNA stability and translation efficiency. Sequences flanking the AUG start codon within an mRNA can influence its recognition by eukaryotic ribosomes. A consensus Kozak sequence has been shown to be important and required for the optimal translation of mammalian genes (13, 14). A second point at which efficiency of translation can be improved is by optimisation of codon usage. Codon bias is observed in many species with the greatest deviation from random codon usage seen in highly expressed genes. Optimisation of codon usage for the species in which the transgene is expressed has resulted in significantly higher levels of protein expression, particularly when expressing viral proteins for genetic vaccination purposes (13, 15, 16). Microdystrophin cDNAs used in this study were modified to include a consensus Kozak

sequence, codon usage was modified based on tRNA frequencies in human, and GC content was increased to promote mRNA stability (17). We have demonstrated that by optimising the cDNA sequence of a eukaryotic gene for expression in a eukaryotic system, levels of mRNA can be significantly increased, as can the number of dystrophin positive fibres following intramuscular plasmid gene transfer and systemic rAAV gene transfer. This observation is in accordance with recent data which demonstrate optimised protein expression of eukaryotic genes through either incorporation of a Kozak sequence (18) or codon optimisation (19).

Although mRNA levels from both codon-optimised constructs are equivalent, levels of protein expression seen following both plasmid and rAAV gene transfer was much higher with microdystrophin ΔR4-R23/ΔCT than ΔAB/R3-R18/ΔCT (through increased numbers of fibres and over expression within individual fibres). Transfection of skeletal muscle fibres with each of the microdystrophin constructs whether by viral or non-viral vectors should be equally efficient, and as mRNA production from both plasmids also appears to be equal, the difference in levels of protein expression may be attributed to protein stability. This is manifest at 1 week post electrotransfer as accumulation of microdystrophin ΔR4-R23/ΔCT within the cytoplasm of transfected fibres, although at this time point equal numbers of positive fibres were observed. By 8 weeks post rAAV gene transfer higher numbers of microdystrophin positive fibres are observed in the ΔR4-R23/ΔCT treated group compared to codon-optimised ΔAB/R3-R18/ΔCT. This difference may be due to the loss of ΔAB/R3-R18/ΔCT fibres over time as a result of lower bio-functionality of the protein or protein instability.

rAAV is a non-pathogenic, replication defective parvovirus, which is being extensively investigated as a gene delivery vehicle due to its apparent ability to exhibit prolonged transgene expression in the absence of an immune response. Many different serotypes of AAV have been described (20-22). Of relevance to DMD are those which show very high tropism for skeletal and cardiac muscles and in particular are able to transduce these tissues following systemic administration. A number of groups have demonstrated this effect with rAAV serotypes 6, 8 and 9 (7, 12, 23, 24). Although very dramatic levels of gene transfer were achieved in these studies, high titres of rAAV were required to achieve these levels of transduction (7). Scaling up these doses to larger animal models and humans involves technical issues; in terms of manufacturing large enough batches of virus and avoiding immune complications associated with delivery of such large viral doses. Optimisation of cDNA sequences for gene therapy may be one way to reduce the viral dose required for efficient gene transfer.

rAAV vector serotypes 8 and 9 are of particular interest for gene therapy of DMD due to their ability to transduce both cardiac and skeletal muscle. Although skeletal muscle is initially the primary clinical feature of DMD, cardiac and respiratory failure are the main causes of morbidity in these patients. Recent data from transgenic mdx mice that express dystrophin in skeletal muscle but not cardiac muscle demonstrated a five fold increase in cardiac injury (25), most likely due to increased activity in these mice, underlying the importance of treating both cardiac and skeletal muscle in DMD patients.

Optimisation of microdystrophin ΔR4-R23/ΔCT cDNA resulted in high levels of expression of microdystrophin in both cardiac and some skeletal muscles following systemic administration of $3x10^{11}$vg rAAV2/8. Comparable studies where $3x10^{11}$vg of rAAV2/8 CMV LacZ vectors have been administered via the same route, have similarly achieved good levels of expression in the heart, but very low levels of transduced fibres in skeletal muscle (12, 23). In contrast to these studies, we demonstrate that we can achieve significant levels of microdystrophin expression in cardiac and skeletal muscles under the control of the muscle restrictive promoter Spc5-12 following an equivalent dose of rAAV2/8. It should be noted that this dose of rAAV2/8 did not achieve the body wide skeletal muscle gene expression previously demonstrated with much higher doses ($7.2x10^{12}$vg) of rAAV8 (12), but is encouraging that cardiac and skeletal muscle systemic gene transfer may be achieved with much lower doses than has previously been required, particularly in conjunction with serotypes such as rAAV9 which exhibit higher tropism for muscle cells (23, 26).

The second aim of the study was to compare the functional properties of the optimised microdystrophin cDNA's. Expression of non-optimised AB/R3-R18/ΔCT in neonatal mdx muscle (following i.m. injection) had no impact on the progression of the dystrophic pathology, however optimised microdystrophin AB/R3-R18/ΔCT improved specific force compared to untreated mdx muscle. This improvement is likely to be due to the increase in number of dystrophin positive fibres, but this did not result in any improvement in muscle pathology markers such as central nucleation. In comparison, expression of microdystrophin ΔR4-R23/ΔCT was able to completely prevent the onset of dystrophic pathology in mdx mice by all parameters tested. The configuration of microdystrophin

ΔR4-R23/ΔCT is based upon a microdystrophin described by the Chamberlain group (8). This construct has previously been shown to be highly functional, demonstrating improvements in both muscle function and muscle pathology, following gene transfer to neonatal, young and old mdx mice (6, 7, 11, 27). In comparable studies where mdx mice have been treated with rAAV as neonates (10, 27), specific force and levels of central nucleation have been improved, with minimal improvements observed in resistance to eccentric contractions. Despite 10 fold fewer viral genomes being administered in the current study, we demonstrate complete normalisation of specific force and levels of central nucleation. We also demonstrate a substantial improvement in protection from eccentric contractions, using a protocol more physiologically relevant to the protocol employed by Banks et at (10). As the rAAV microdystrophin vectors used by the Chamberlain group have essentially the same configuration including an optimal Kozak sequence (8), the improved outcome that we observe may be a reflection of the increased levels of dystrophin fibres and protein, as a result of codon optimisation and the use of highly efficient serotype rAAV2/8 vectors.

For the first time this study directly compares the functionality of two previously described microdystrophin configurations (4, 8). Whilst codon optimisation improved the functional outcome following treatment with rAAV2/8 AB/R3-R18/ΔCT, it is clear that microdystrophin ΔR4-R23/ΔCT is more functionally protective against the pathological changes that occur in mdx muscle. One possible explanation for this difference is the higher number of dystrophin positive fibres observed in these mice, as recovery of muscle function in mdx mice may be related to the number of dystrophin positive fibres and the levels of dystrophin expression within the muscle.

The reduced function of microdystrophin ΔAB/R3-R18/ΔCT may also be attributed to deletions within the actin binding domain 1 (ABD1) at the N-terminus of the protein, which microdystrophin ΔR4-R23/ΔCT does not have. Full length dystrophin has two ABD domains, ABD1 at the N-terminus of the protein and ABD2 within the rod domain. Studies in transgenic mice have demonstrated that the lack of both ABDs leads to a severe dystrophic phenotype (28), whilst deletion of a single ABD, including the deletion included in microdystrophin ΔAB/R3-R18/ΔCT can lead to a relatively mild phenotype (1, 29-31). We have shown previously that this microdystrophin can lead to histological improvements in the dystrophic phenotype of mdx mice (4), but the combination of deletions in ABD1 and of the entire ABD2 may provide insufficient actin binding to achieve functional stability at the levels observed with microdystrophin ΔR4-R23/ΔCT. This is supported by the recent study of Banks et al which studied the effects of deletions in ABD1 of a microdystrophin with the same configuration as ΔR4-R23/ΔCT (10), although, in contrast to our study, there was no observed improvement in either specific force or resistance to eccentric contractions.

The lower functional capacity of microdystrophin ΔAB/R3-R18/ΔCT may also explain why we observe much lower numbers of dystrophin positive fibres at 8 weeks post injection compared to microdystrophin ΔR4-R23/ΔCT. Quantitative RT-PCR analysis showed that mRNA levels were increased equally by codon optimisation of these constructs; we would have expected to see equal levels of dystrophin expression but at 8 weeks post injection this was not the case. It is possible that the number of dystrophin

positive fibres were initially equivalent (as observed following plasmid gene transfer), but declined in rAAV2/8 ΔAB/R3-R18/ΔCT treated mice due to incomplete protection against necrosis and degeneration of dystrophin positive fibres. A similar effect was observed by Banks et al following neonatal administration of microdystrophins containing ABD1 deletions (10).

We conclude that optimisation of microdystrophin cDNA sequences for codon usage, GC content and the inclusion of optimal Kozak sequences, can significantly improve the outcome of gene transfer studies through maximising gene expression and protein levels. This system will be applicable to both viral gene transfer in allowing effective viral doses to be reduced and increasing the efficiency of vector production (19), and also in improving efficiency of non viral gene transfer not only to muscle but across the whole field of gene therapy.

Materials and Methods:

Generation of constructs

Non codon-optimised human microdystrophin ΔAB/R3-R18/ΔCT was constructed as previously described (4). Codon-optimised cDNA sequences of human and murine microdystrophins ΔAB/R3-R18/ΔCT and ΔR4-R23/ΔCT were generated by Geneart (Regensburg, Germany). These cDNA sequences, including an optimal Kozak sequence, were cloned into a pDD derived AAV plasmid (32) under the control of the muscle restrictive promoter Spc5-12 (33). HEK293T cells were transfected with the expression plasmid and the helper plasmids pAdΔF6 and pAAV5E18-VD2/8 (J. Wilson, University of Pennsylvania, USA) by means of calcium phosphate precipitation (34). Cell pellets were harvested and lysed in 50mM Tris-Cl, 150mM NaCl. Lysates were clarified by centrifugation at 6700rpm for 20 mins and passed through a 0.45μm filter. Cell lysates were layered on an iodixanol gradient (Sigma-Aldrich, Poole, UK,) and centrifuged at 60,000rpm for 90 mins. The 40% iodixanol layer containing the viral particles was isolated, concentrated with PBS, 5mM $MgCl_2$, 12.5mM KCl (PBS-MK), through a Amicon Ultra 15 100KDa (Millipore UK). The number of vector genomes was determined relative to a plasmid DNA standard using Dot blot hybridization.

Tissue culture and qRT-PCR

HEK293T cells were grown and maintained in DMEM, 10%FCS at 8% CO_2 in a humidified incubator. Cells were seeded at a density of $1x10^4$ cells/cm^2 in a 6 well plate and transfected with 4μg plasmid DNA (pΔAB/R3-R18/ΔCT, codon-optimised pΔAB/R3-R18/ΔCT or pΔR4-R23/ΔCT) using Lipofectamine 2000 (Invitrogen, Paisley, UK). All transfections were carried out in quadruplicate. Cells were harvested after 48 hours and RNA was extracted using an RNeasy Kit (Qiagen, Crawley, UK).

Total RNA (1μg) was reverse transcribed in a final volume of 25μl containing 5μl 5x RT buffer, 25U RNasin RNase inhibitor, 5μl 10mM dNTP, 200U M-MLV Reverse Transcriptase (Promega, Southampton, UK) and 2.5μM random nonamers (Sigma). Reactions were incubated at 42°C for 60 min and reverse transcriptase was inactivated by heating at 70°C for 15 min and cooling at 4°C for 5 min.

Specific primer sets were as follows (5'→3'): for microdystrophin, AACAAAGTGCCCTACTA (forward) and AGGTTGTGCTGGTCCA (reverse); for ribosomal RNA 18S TTGACGGAAGGGCACCACCAG (forward) and GCACCACCACCCACGGAATCG (reverse). For each experiment a reaction mix was prepared; for each tube 2.5μl forward primer (20nM), 2.5μl reverse primer (20nM), 2.5μl RNAse-free DNAse-free water and 12.5μl SYBR Green Master Mix (Eurogentec Southampton, UK). Aliquots (20μl) of this mix were placed in the SmartCycler tubes and 5μl cDNA solution was added to each reaction. All reactions were processed in duplicate. The experimental run protocol was: denaturation (95°C for 10 min) and 40 cycles of 95°C for 15s, 60°C for 30s, 72°C for 30s with a single fluorescence

measurement. Melting curve program (60-95°C with heating at 0.1°C per second and continuous fluorescence measurement). mRNA concentrations were normalised to that of the ribosomal 18S RNA in each sample.

Administration of rAAV

Wild type C57Bl/10 and mdx mice were housed in minimal disease facilities (Royal Holloway, University of London and Imperial College London) with food and water *ad libitum.* For physiological studies 5 day old neonatal mdx mice were anaesthetised by indirect contact with ice and injected intra-muscularly with $7.5x10^9$ vector genomes (vg) of rAAV expressing human microdystrophins in 5μl PBS-MK. Physiological and histological assessment was performed at 8 weeks post administration of rAAV. Systemic administration of rAAV was performed in 10 week old mdx mice. Mice were restrained and $3x10^{11}$ vg in 100μl of PBS-MK of rAAV expressing microdystrophins were injected via the tail vein. Histological analysis was performed at 12 weeks post administration of rAAV.

Electrotransfer of plasmid DNA

Two hours prior to the injection of plasmid DNA, 25μl of bovine hyaluronidase (Sigma) solution (10U) was injected intra-muscularly into the TA muscle of 6-8 week old mdx mice, under fentanyl/fluanisone (VetaPharma Ltd, Leeds, UK) and midazolam (Roche, Lewes, UK) general anaesthesia. Immediately after the injection of 25μg plasmid DNA

into the TA, electrotransfer was carried out as follows: Using a BTX 830 electroporator with Tweezertrodes (Genetronics, San Diego, USA) electric pulses were applied to the mouse hind limb. Electrodes were placed in medial and lateral positions relative to the TA. For each treatment, a voltage of 175V/cm was applied in ten pulses of 20ms each, at a frequency of 1Hz. Each TA muscle was measured prior to electrotransfer so that voltage could be adjusted accordingly. Electrotransfer was performed under isoflurane gaseous anaesthetic.

Histology

Recovered tissues were mounted in Cryo-M-Bed (Bright Instruments, Huntingdon, UK) and snap frozen in liquid nitrogen cooled isopentane. Dystrophin staining was carried out on 10μm cryosections. Frozen tissue sections from control and treated mice were air dried for 30mins and blocked using an avidin/biotin blocking kit and Mouse on Mouse kit (Vector Ltd, Peterborough, UK). Microdystrophin was detected with a primary antibody (at a dilution 1/50) against repeat region 1 of the rod domain (MANEX 1011C, Glenn Morris, Oswestry, UK). Sections were incubated with primary antibody for 30 minutes and then washed in PBS. Immunostaining was completed using secondary antibody and avidin/biotin amplification system from Mouse on Mouse kit. Dystrophin staining was visualised using 3,3'-diaminobenzidine (Vector Ltd.).

To assess central nucleation and pathology muscles were stained with haematoxylin and eosin. Cryosections were air dried for 30 minutes and stained with Mayer’s

haematoxylin (Sigma) for 1 minute and washed in tap water for 3 minutes. Sections were counterstained with 1% eosin (VWR, Lutterworth, UK) for 5 minutes. Sections were dehydrated in 100% ethanol, cleared in xylene and mounted in DPX (VWR). To assess central nucleation three random areas were assessed in each treated and control (mdx and wild type) mouse (n=6 per group). The total number of fibres in these areas was counted and the number of centrally nucleated fibres was expressed as a percentage of the total number of fibres. To assess numbers of dystrophin positive fibres, the number of positive fibres was counted in four random fields of a muscle section and the average number per field was calculated for each muscle.

In situ muscle function and lengthening contraction protocol

Mice were anaesthetised with an intra-peritoneal injection of fentanyl/fluanisone, midazolam and water (1:1:2 by vol.) at a dosage of 10ml/kg. The mice were carefully monitored throughout the experiment and additional doses of anaesthetic were administered to ensure that there was no reflex response to toe pinch. Under deep anaesthesia the distal tendon of the tibialis anterior (TA) muscle was dissected from surrounding tissue and the tendon tied with 4.0 braided surgical silk. The sciatic nerve was exposed and all its branches cut except for the common peroneal nerve (CPN), which innervates the TA muscle. The mouse was placed on a thermopad (Harvard Apparatus) to maintain body temperature at 37ºC. The foot was secured to a platform and the ankle and knee immobilized using stainless steel pins. The TA tendon was attached to the lever arm of a 305B dual-mode servomotor transducer (Aurora Scientific Inc., Ontario, Canada) via a custom made steel s-hook.

TA muscle contractions were elicited by stimulating the distal part of CPN via bipolar platinum electrodes, using supramaximal square-wave pulses of 0.02 ms (701A stimulator; Aurora Scientific Inc). Data acquisition and control of the servomotors were conducted using a Lab-View based DMC program (Dynamic muscle control and Data Acquisition; Aurora Scientific, Inc.). Optimal muscle length (L_o) was determined by incrementally stretching the muscle using micromanipulators until the maximum isometric twitch force was achieved. Maximum isometric tetanic force (P_o) was determined from the plateau of the force-frequency relationship following a series of stimulations at 10, 30, 40, 50, 80, 100, 120, 150, and 180 Hz. A one minute rest period was allowed between each tetanic contraction. Muscle length was measured using digital calipers based on well defined anatomical landmarks near the knee and the ankle. The specific force (N/cm^2) was calculated by dividing P_o by TA muscle cross-sectional area (CSA). Overall CSA was estimated using the following formula: muscle weight (g) / [L_o (cm) x 1.06 (g/cm^3).

After establishing the force-frequency relationship, the susceptibility of TA muscles to eccentric contraction-induced injury was assessed. This consisted of stimulating the muscle at 180 Hz (the frequency that usually resulted in P_o) for 700 ms. After 500 ms of stimulation the muscle was lengthened by 10% of L_o at a velocity of 0.5 L_o s/1. At the end of stimulation the muscle was returned to L_o at a rate of -0.5 L_o s/1. The stimulation-stretch cycle was repeated every 3 min for a total of 10 cycles. The rest time between each cycle limited the potential for developing muscle fatigue. Maximum isometric force was measured after each eccentric contraction and expressed as a percentage of the

initial maximum isometric force. At the end of the experiment the muscles were excised, weighed and prepared for histological analysis.

Statistical Analysis

All data are presented as mean values ±SEM (cohort size stated per experiment). All statistical analysis was performed by one way ANOVA followed by Tukey-Kramer post-hoc analysis.

Acknowledgements:

We are grateful to Julie Johnston and James Wilson of the University of Pennsylvania for supplying plasmids vectors to allow AAV2/8 viral production, Ruxandra Draghia-Akli, VGX Pharmaceuticals for supplying the Spc5-12 promoter and to Glenn Morris at the Centre for Inherited Neuromuscular Disease for supplying monoclonal antibody MANEX1011c to detect dystrophin. This work was funded by grants from the Muscular Dystrophy Campaign, Association Francais contre les Myopathies, EU FP6 MOLEDA STREP and EU FP6 Clinigene Network of Excellence.

References:

1. Wells, D.J., Wells, K.E., Asante, E.A., Turner, G., Sunada, Y., Campbell, K.P., Walsh, F.S. and Dickson, G. (1995) Expression of human full-length and minidystrophin in transgenic mdx mice: implications for gene therapy of Duchenne muscular dystrophy. *Hum Mol Genet,* 4, 1245-50.
2. Neri, M., Torelli, S., Brown, S., Ugo, I., Sabatelli, P., Merlini, L., Spitali, P., Rimessi, P., Gualandi, F., Sewry, C. *et al.* (2007) Dystrophin levels as low as 30% are sufficient to avoid muscular dystrophy in the human. *Neuromuscul Disord,* 17, 913-8.
3. Athanasopoulos, T., Graham, I.R., Foster, H. and Dickson, G. (2004) Recombinant adeno-associated viral (rAAV) vectors as therapeutic tools for Duchenne muscular dystrophy (DMD). *Gene Ther,* 11 Suppl 1, S109-21.
4. Fabb, S.A., Wells, D.J., Serpente, P. and Dickson, G. (2002) Adeno-associated virus vector gene transfer and sarcolemmal expression of a 144 kDa micro-dystrophin effectively restores the dystrophin-associated protein complex and inhibits myofibre degeneration in nude/mdx mice. *Hum Mol Genet,* 11, 733-41.
5. Gregorevic, P., Allen, J.M., Minami, E., Blankinship, M.J., Haraguchi, M., Meuse, L., Finn, E., Adams, M.E., Froehner, S.C., Murry, C.E. *et al.* (2006) rAAV6-microdystrophin preserves muscle function and extends lifespan in severely dystrophic mice. *Nat Med,* 12, 787-9.
6. Gregorevic, P., Blankinship, M.J., Allen, J.M. and Chamberlain, J.S. (2008) Systemic microdystrophin gene delivery improves skeletal muscle structure and function in old dystrophic mdx mice. *Mol Ther,* 16, 657-64.
7. Gregorevic, P., Blankinship, M.J., Allen, J.M., Crawford, R.W., Meuse, L., Miller, D.G., Russell, D.W. and Chamberlain, J.S. (2004) Systemic delivery of genes to striated muscles using adeno-associated viral vectors. *Nat Med,* 10, 828-34.
8. Harper, S.Q., Hauser, M.A., DelloRusso, C., Duan, D., Crawford, R.W., Phelps, S.F., Harper, H.A., Robinson, A.S., Engelhardt, J.F., Brooks, S.V. *et al.* (2002) Modular flexibility of dystrophin: implications for gene therapy of Duchenne muscular dystrophy. *Nat Med,* 8, 253-61.
9. Watchko, J., O'Day, T., Wang, B., Zhou, L., Tang, Y., Li, J. and Xiao, X. (2002) Adeno-associated virus vector-mediated minidystrophin gene therapy improves dystrophic muscle contractile function in mdx mice. *Hum Gene Ther,* 13, 1451-60.
10. Banks, G.B., Gregorevic, P., Allen, J.M., Finn, E.E. and Chamberlain, J.S. (2007) Functional capacity of dystrophins carrying deletions in the N-terminal actin-binding domain. *Hum Mol Genet,* 16, 2105-13.
11. Liu, M., Yue, Y., Harper, S.Q., Grange, R.W., Chamberlain, J.S. and Duan, D. (2005) Adeno-associated virus-mediated microdystrophin expression protects young mdx muscle from contraction-induced injury. *Mol Ther,* 11, 245-56.
12. Nakai, H., Fuess, S., Storm, T.A., Muramatsu, S., Nara, Y. and Kay, M.A. (2005) Unrestricted hepatocyte transduction with adeno-associated virus serotype 8 vectors in mice. *J Virol,* 79, 214-24.
13. Garmory, H.S., Brown, K.A. and Titball, R.W. (2003) DNA vaccines: improving expression of antigens. *Genet Vaccines Ther,* 1, 2.

14. Kozak, M. (2005) Regulation of translation via mRNA structure in prokaryotes and eukaryotes. *Gene,* 361, 13-37.
15. Koldej, R., Cmielewski, P., Stocker, A., Parsons, D.W. and Anson, D.S. (2005) Optimisation of a multipartite human immunodeficiency virus based vector system; control of virus infectivity and large-scale production. *J Gene Med,* 7, 1390-9.
16. Michel, M., Lone, Y.C., Centlivre, M., Roux, P., Wain-Hobson, S. and Sala, M. (2007) Optimisation of secretion of recombinant HBsAg virus-like particles: Impact on the development of HIV-1/HBV bivalent vaccines. *Vaccine,* 25, 1901-11.
17. Murray, E.L. and Schoenberg, D.R. (2007) A+U-rich instability elements differentially activate 5'-3' and 3'-5' mRNA decay. *Mol Cell Biol,* 27, 2791-9.
18. Bennicelli, J., Wright, J.F., Komaromy, A., Jacobs, J.B., Hauck, B., Zelenaia, O., Mingozzi, F., Hui, D., Chung, D., Rex, T.S. *et al.* (2008) Reversal of blindness in animal models of leber congenital amaurosis using optimized AAV2-mediated gene transfer. *Mol Ther,* 16, 458-65.
19. Radcliffe, P.A., Sion, C.J., Wilkes, F.J., Custard, E.J., Beard, G.L., Kingsman, S.M. and Mitrophanous, K.A. (2008) Analysis of factor VIII mediated suppression of lentiviral vector titres. *Gene Ther,* 15, 289-97.
20. Gao, G., Vandenberghe, L.H., Alvira, M.R., Lu, Y., Calcedo, R., Zhou, X. and Wilson, J.M. (2004) Clades of Adeno-associated viruses are widely disseminated in human tissues. *J Virol,* 78, 6381-8.
21. Gao, G., Vandenberghe, L.H. and Wilson, J.M. (2005) New recombinant serotypes of AAV vectors. *Curr Gene Ther,* 5, 285-97.
22. Gao, G.P., Alvira, M.R., Wang, L., Calcedo, R., Johnston, J. and Wilson, J.M. (2002) Novel adeno-associated viruses from rhesus monkeys as vectors for human gene therapy. *Proc Natl Acad Sci U S A,* 99, 11854-9.
23. Inagaki, K., Fuess, S., Storm, T.A., Gibson, G.A., McTiernan, C.F., Kay, M.A. and Nakai, H. (2006) Robust systemic transduction with AAV9 vectors in mice: efficient global cardiac gene transfer superior to that of AAV8. *Mol Ther,* 14, 45-53.
24. Wang, Z., Zhu, T., Qiao, C., Zhou, L., Wang, B., Zhang, J., Chen, C., Li, J. and Xiao, X. (2005) Adeno-associated virus serotype 8 efficiently delivers genes to muscle and heart. *Nat Biotechnol,* 23, 321-8.
25. Townsend, D., Yasuda, S., Li, S., Chamberlain, J.S. and Metzger, J.M. (2008) Emergent dilated cardiomyopathy caused by targeted repair of dystrophic skeletal muscle. *Mol Ther,* 16, 832-5.
26. Zincarelli, C., Soltys, S., Rengo, G. and Rabinowitz, J.E. (2008) Analysis of AAV serotypes 1-9 mediated gene expression and tropism in mice after systemic injection. *Mol Ther,* 16, 1073-80.
27. Yoshimura, M., Sakamoto, M., Ikemoto, M., Mochizuki, Y., Yuasa, K., Miyagoe-Suzuki, Y. and Takeda, S. (2004) AAV vector-mediated microdystrophin expression in a relatively small percentage of mdx myofibers improved the mdx phenotype. *Mol Ther,* 10, 821-8.
28. Judge, L.M., Haraguchiln, M. and Chamberlain, J.S. (2006) Dissecting the signaling and mechanical functions of the dystrophin-glycoprotein complex. *J Cell Sci,* 119, 1537-46.

29. Phelps, S.F., Hauser, M.A., Cole, N.M., Rafael, J.A., Hinkle, R.T., Faulkner, J.A. and Chamberlain, J.S. (1995) Expression of full-length and truncated dystrophin mini-genes in transgenic mdx mice. *Hum Mol Genet,* 4, 1251-8.
30. Warner, L.E., DelloRusso, C., Crawford, R.W., Rybakova, I.N., Patel, J.R., Ervasti, J.M. and Chamberlain, J.S. (2002) Expression of Dp260 in muscle tethers the actin cytoskeleton to the dystrophin-glycoprotein complex and partially prevents dystrophy. *Hum Mol Genet,* 11, 1095-105.
31. Corrado, K., Rafael, J.A., Mills, P.L., Cole, N.M., Faulkner, J.A., Wang, K. and Chamberlain, J.S. (1996) Transgenic mdx mice expressing dystrophin with a deletion in the actin-binding domain display a "mild Becker" phenotype. *J Cell Biol,* 134, 873-84.
32. Yue, Y. and Dongsheng, D. (2002) Development of multiple cloning site cis-vectors for recombinant adeno-associated virus production. *Biotechniques,* 33, 672, 674, 676-8.
33. Li, X., Eastman, E.M., Schwartz, R.J. and Draghia-Akli, R. (1999) Synthetic muscle promoters: activities exceeding naturally occurring regulatory sequences. *Nat Biotechnol,* 17, 241-5.
34. Liu, Y.L., Wagner, K., Robinson, N., Sabatino, D., Margaritis, P., Xiao, W. and Herzog, R.W. (2003) Optimized production of high-titer recombinant adeno-associated virus in roller bottles. *Biotechniques,* 34, 184-9.

Figure Legends:

Figure 1 Codon optimisation of microdystrophin increases mRNA and protein levels following plasmid gene transfer.

(a) Quantitative RT-PCR of microdystrophin mRNA 48 hours post transfection of HEK293T cells. Levels of microdystrophin mRNA are expressed relative to the housekeeping gene Ribosome18S. (b) Total number of microdystrophin positive fibres at 7 days post electrotransfer of 25μg plasmid DNA in TA of mdx mice (6-8 week old). (c&d) Dystrophin staining using MANEX1011C in treated TA muscles (c) codon-optimised ΔAB/R3-R18/ΔCT (d) codon-optimised ΔAB/R3-R18/ΔCT. Error bars are mean ± s.e.m (n=4, * $p<0.05$ compared to non codon-optimised ΔAB/R3-R18/ΔCT). Scale bar = 300μm.

Figure 2 Efficient cardiac gene transfer following systemic administration of codon-optimised microdystrophin.

Average number of microdystrophin positive cardiomyocytes within a field of myocardium following administration of $3x10^{11}$vg AAV8 microdystrophin via the tail vein of 10 week old mdx mice. Analysis was performed 12 weeks post- injection. Error bars shown as mean ±s.e.m (n=4). *$p<0.001$ compared to non-codon-optimised ΔAB/R3-R18/ΔCT, **$p<0.001$ compared to non-codon-optimised ΔAB/R3-R18/ΔCT and codon-optimised ΔAB/R3-R18/ΔCT.

Figure 3 Expression of codon-optimised ΔR4-R23/ΔCT microdystrophin following systemic administration rAAV2/8 vectors.

Tissue sections were stained for codon-optimised ΔR4-R23/ΔCT microdystrophin expression using monoclonal antibody MANEX1011C (1/50). Scale bar = 300μm

Figure 4 Codon-optimisation of microdystrophin leads to increased numbers of dystrophin positive fibres following intramuscular injection of rAAV2/8 vectors.

TA muscles of neonatal (5 day old) mdx mice were injected with $7.5x10^9$vg rAAV2/8 microdystrophin and analysed histologically at 8 weeks post injection. Sections were either stained for microdystrophin using the anti-dystrophin antibody MANEX1011C (1/50), or with haematoxylin and eosin. Scale bar = 300μm

Figure 5 Intramuscular delivery of codon-optimised microdystrophin improves morphological properties of mdx muscle.

TA muscles of neonatal (5 day old) mdx mice injected with $7.5x10^9$vg AAV2/8 microdystrophin were (a) assessed histologically at 8 weeks post treatment to determine the percentage of centrally nucleated fibres within the TA muscle (b) and weighed. Error bars shown as mean ±s.e.m. (n=6) *$p<0.05$ compared to mdx, **$p<0.001$ compared to mdx and no significant difference compared to C57bl/10.

Figure 6 Intramuscular administration of codon-optimised microdystrophin leads to greater improvements in functional properties of mdx muscle.

TA muscles of neonatal (5 day old) mdx mice injected with $7.5x10^9$vg AAV2/8 microdystrophin were analysed at 8 weeks post injection for their maximal force producing capacity compared to untreated mdx muscle and C57bl/10 age matched controls. Maximal force was also normalised for cross sectional area of the muscle to assess specific force. (a) ΔAB/R3-R21/ΔCT, (b) codon-optimised ΔAB/R3-R21/ΔCT, (c) codon-optimised ΔR4-R23/ΔCT. Error bars shown as mean +/- s.e.m (n=6). *p<0.05 compared to mdx and C57bl/10, **p<0.001 compared to mdx control and no significant difference to C57bl/10.

Figure 7 Intramuscular administration of codon-optimised ΔR4-R23/ΔCT leads to protection from lengthening contractions.

TA muscles of neonatal (5 day old) mdx mice injected with $7.5x10^9$vg AAV2/8 microdystrophin were analysed at 8 weeks post injection. Treated and control muscles were assessed for force deficit following a series of ten lengthening contractions. Maximal tetanic force following each lengthening contraction is displayed as a percentage of initial maximal tetanic force. (a) ΔAB/R3-R21/ΔCT, (b) codon-optimised ΔAB/R3-R21/ΔCT, (c) codon-optimised ΔR4-R23/ΔCT. Error bars shown as mean +/- s.e.m (n=6). **p<0.001 compared to mdx control and no significant difference to C57bl/10.

Figure1

Click here to download high resolution image

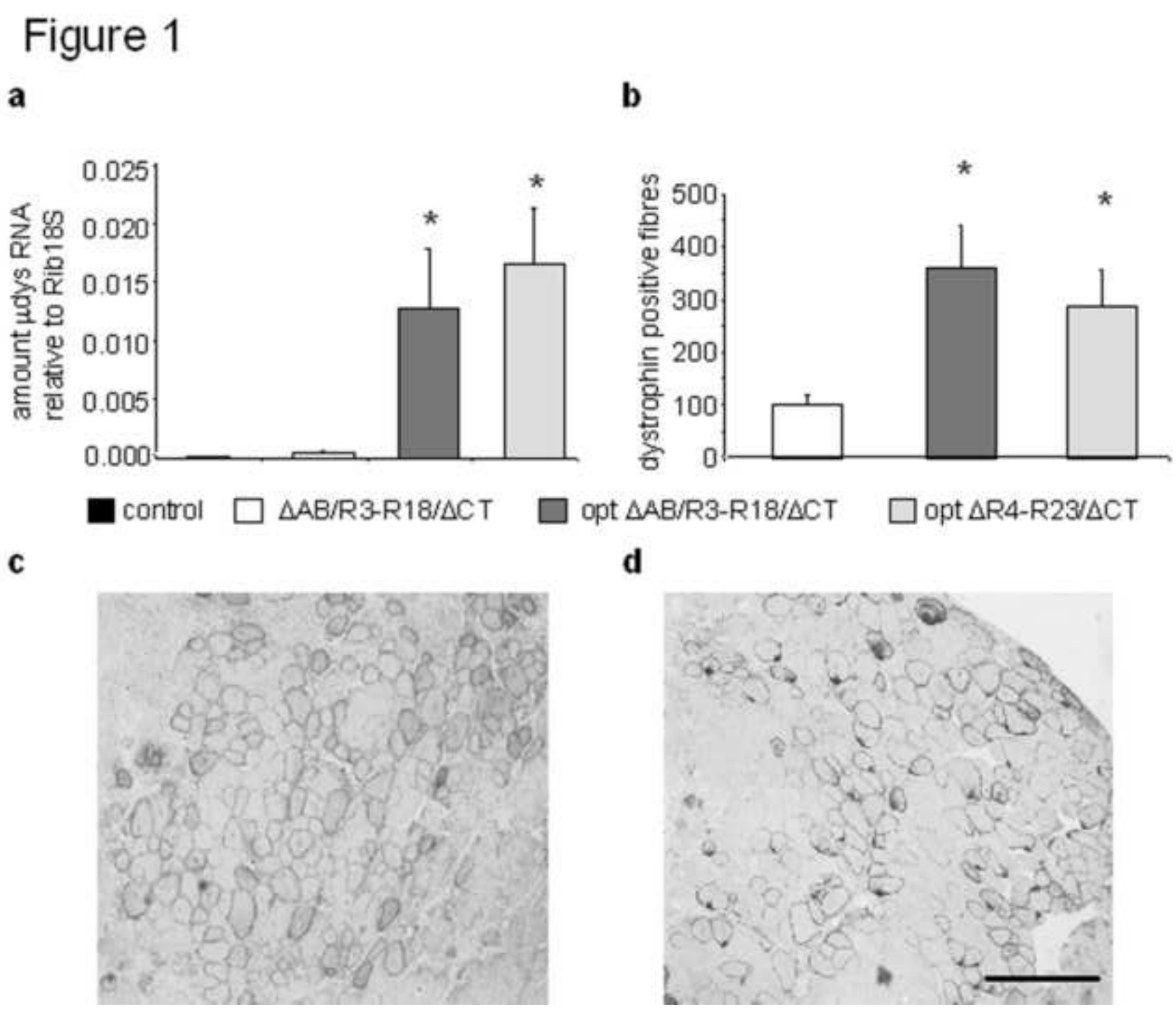

Figure2
Click here to download high resolution image

Figure 2

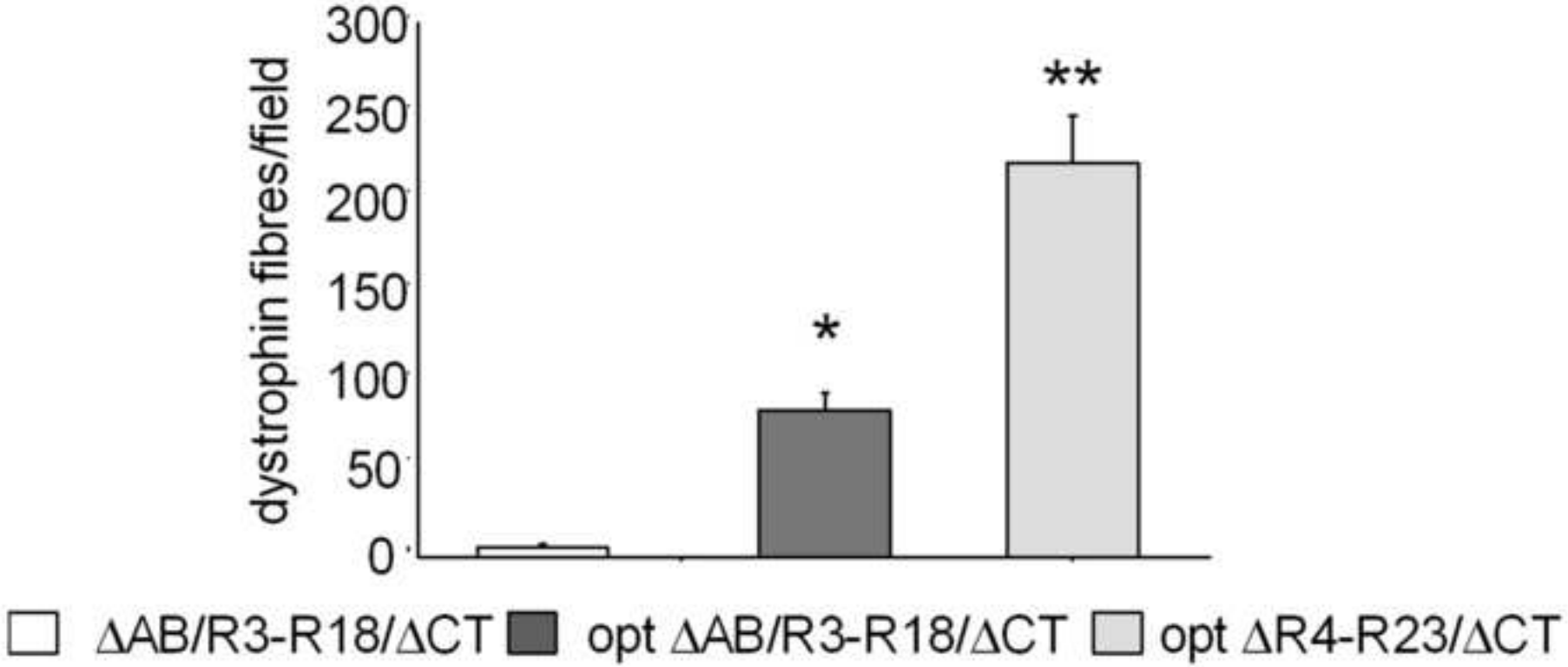

Figure3
Click here to download high resolution image

Figure 3

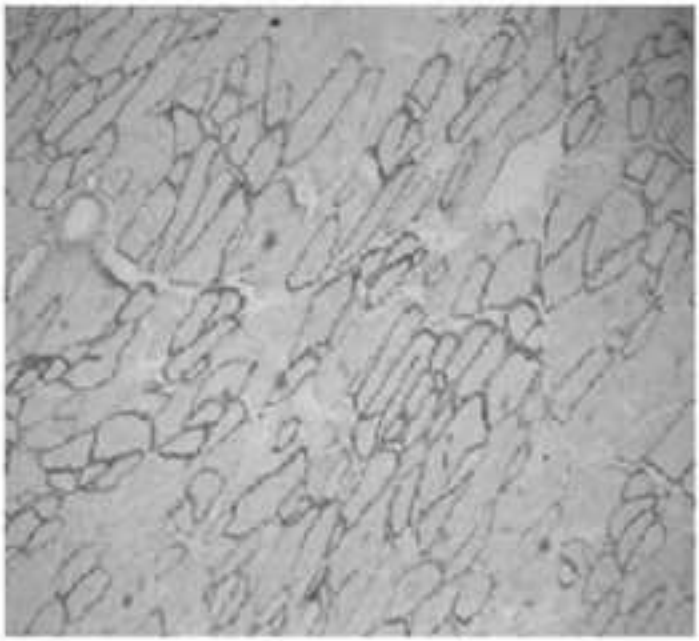

Gastrocnemius

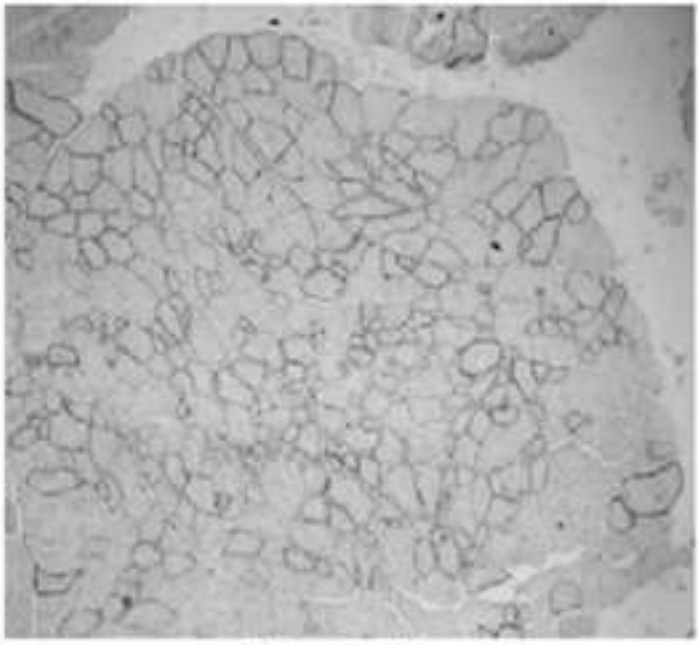

Plantaris

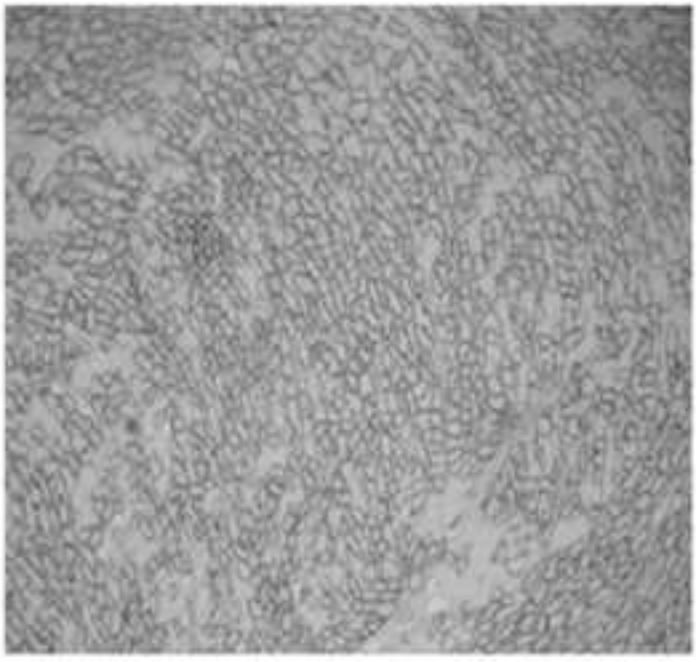

Heart

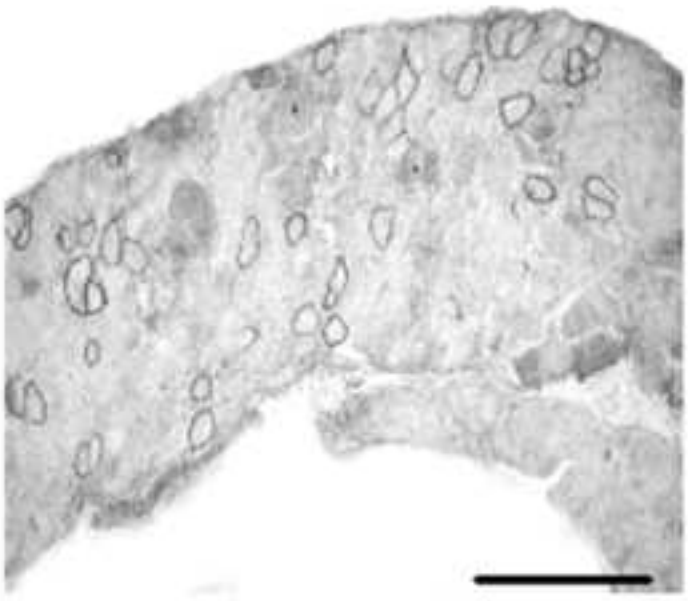

Diaphragm

Figure4

Click here to download high resolution image

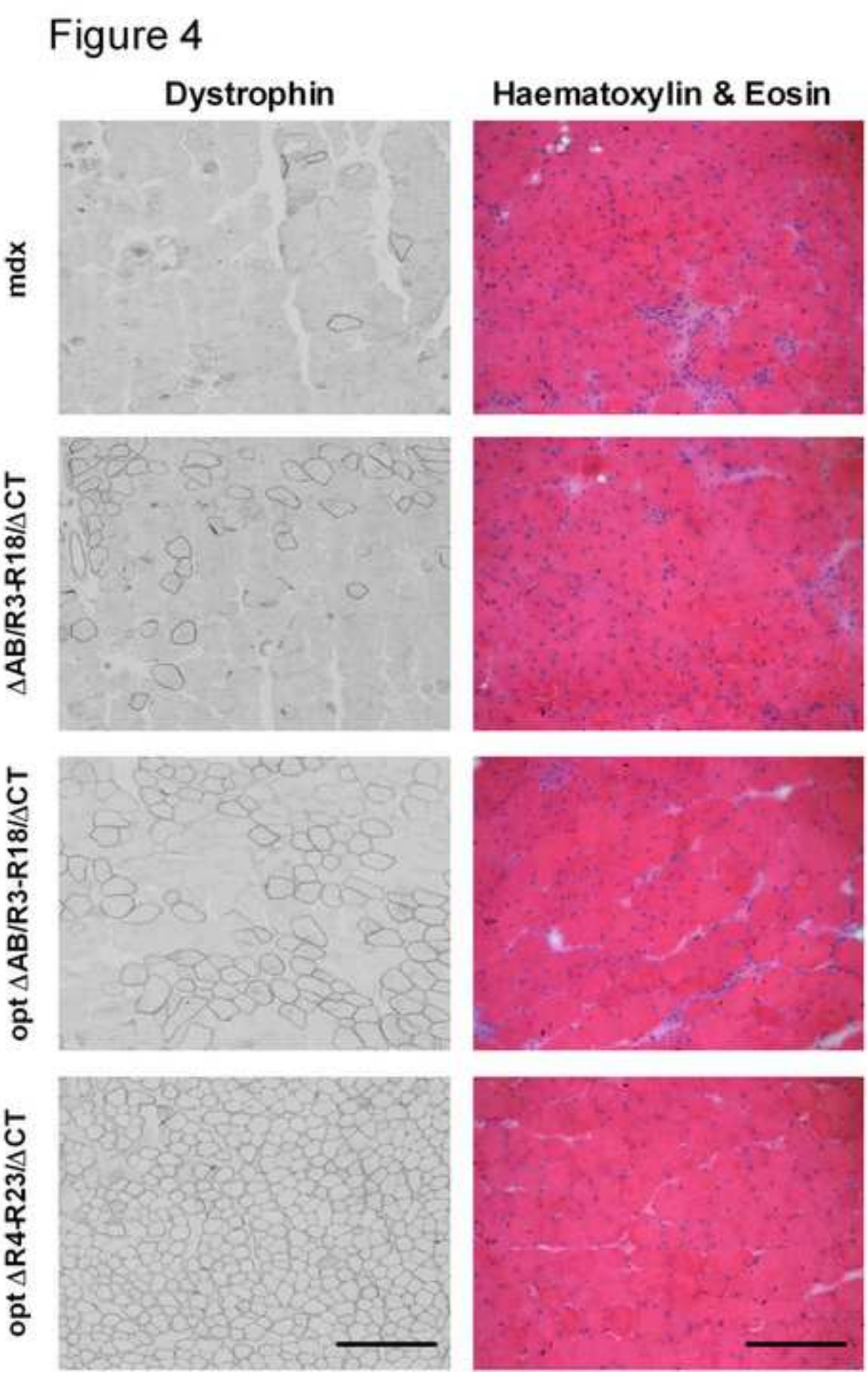

Figure5

Click here to download high resolution image

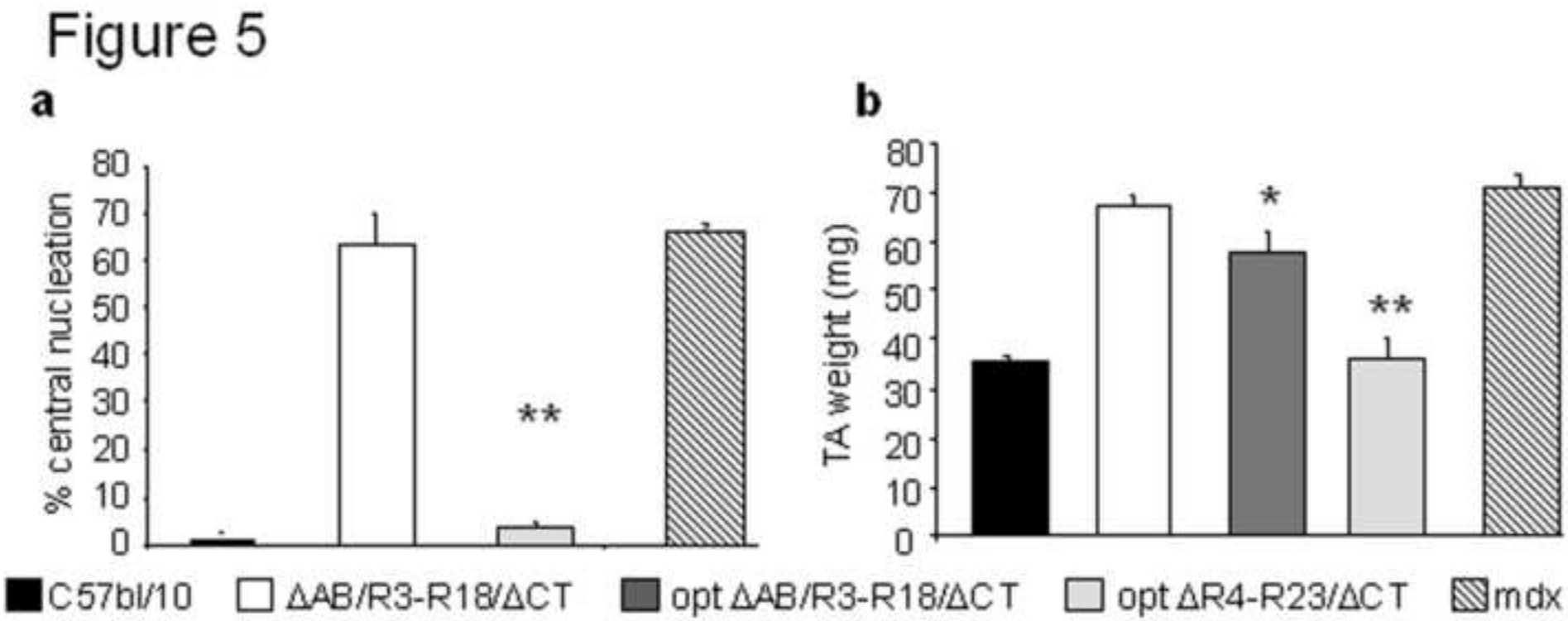

Figure6
Click here to download high resolution image

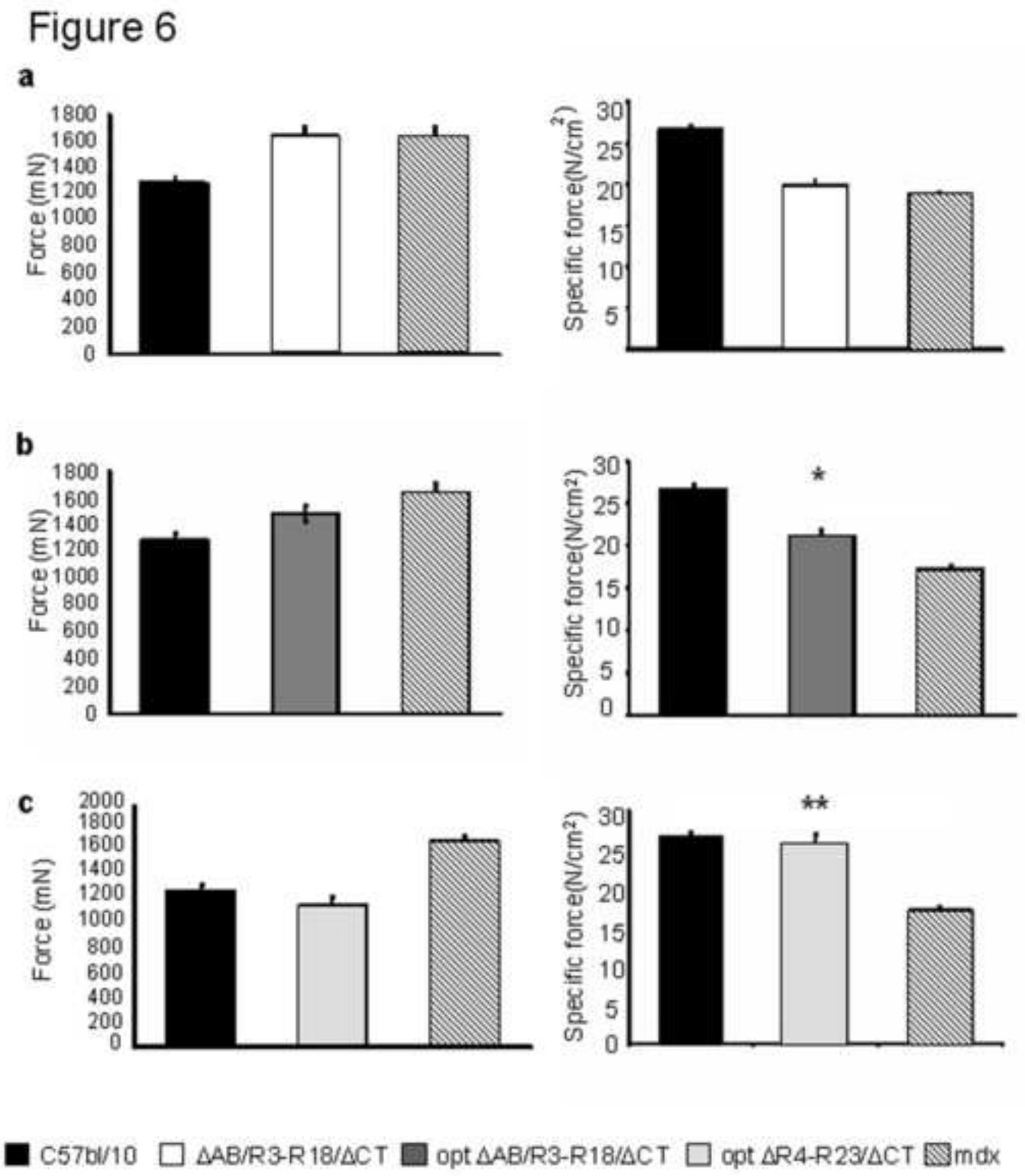

Figure7
Click here to download high resolution image